

# Flux Analysis Uncovers Key Role of Functional Redundancy in Formaldehyde Metabolism

Christopher J. Marx<sup>1‡</sup>, Stephen J. Van Dien<sup>2</sup>, Mary E. Lidstrom<sup>1,3\*</sup>

**1** Department of Microbiology, University of Washington, Seattle, Washington, United States of America, **2** United Metabolics, Seattle, Washington, United States of America, **3** Department of Chemical Engineering, University of Washington, Seattle, Washington, United States of America

**Genome-scale analysis of predicted metabolic pathways has revealed the common occurrence of apparent redundancy for specific functional units, or metabolic modules. In many cases, mutation analysis does not resolve function, and instead, direct experimental analysis of metabolic flux under changing conditions is necessary. In order to use genome sequences to build models of cellular function, it is important to define function for such apparently redundant systems. Here we describe direct flux measurements to determine the role of redundancy in three modules involved in formaldehyde assimilation and dissimilation in a bacterium growing on methanol. A combination of deuterium and <sup>14</sup>C labeling was used to measure the flux through each of the branches of metabolism for growth on methanol during transitions into and out of methylotrophy. The cells were found to differentially partition formaldehyde among the three modules depending on the flux of methanol into the cell. A dynamic mathematical model demonstrated that the kinetic constants of the enzymes involved are sufficient to account for this phenomenon. We demonstrate the role of redundancy in formaldehyde metabolism and have uncovered a new paradigm for coping with toxic, high-flux metabolic intermediates: a dynamic, interconnected metabolic loop.**

Citation: Marx CJ, Van Dien SJ, Lidstrom ME (2005) Flux analysis uncovers key role of functional redundancy in formaldehyde metabolism. PLoS Biol 3(2): e16.

## Introduction

The availability of large numbers of genome sequences has facilitated metabolic reconstruction based on predicted gene function, in essence, a prediction of the metabolic blueprint of a cell. Such metabolic reconstructions [1,2,3] can be grouped in functional segments, or metabolic modules [4,5], and the compilation of metabolic modules can be used to predict interactions between the different elements of the metabolic network in a cell. However, a major difficulty with this approach is the common occurrence of apparently redundant functional modules. It is often not possible to assign roles to these metabolic segments, which have been referred to as the “gray areas of the genome” [6]. Expression profiling, either of transcripts or proteins, holds the promise to gain more insight into the function of redundant metabolic modules, but the presence of a transcript or protein does not necessarily correlate with module function, due to posttranslational effects on metabolic flux. In order to determine the true function of such metabolic modules, it is necessary to measure the flux of metabolites through each functional module during relevant physiological changes.

One system that has proved amenable to a modular approach to metabolism is the ability to grow on one-carbon (C<sub>1</sub>) compounds, or methylotrophy [7]. The availability of a gapped genome sequence for a model methylotrophic bacterium, *Methylobacterium extorquens* AM1, has accelerated the definition of methylotrophy modules, and a reasonably complete metabolic reconstruction is available for this bacterium [7]. However, these analyses coupled to genetic and physiological studies [8,9,10,11,12,13] have raised a series of fundamental questions that can only be answered through direct flux measurements.

As in other such aerobic methylotrophic bacteria, *M. extorquens* AM1 oxidizes C<sub>1</sub> substrates to formaldehyde and is essentially growing on formaldehyde for both carbon and energy metabolism [14] (Figure 1). It is not yet understood how the toxic central metabolite formaldehyde is efficiently and dynamically partitioned between assimilatory and dissimilatory metabolism, without toxic buildup. Therefore, this system represents both a key problem of methylotrophy and a paradigm for how toxic metabolites are managed in high-flux conditions. Genomic predictions and mutant analyses have identified three functional modules that direct formaldehyde into two outputs: assimilatory or dissimilatory metabolism (Figure 1). The first module consists of the apparently nonenzymatic condensation reaction between formaldehyde and tetrahydrofolate (H<sub>4</sub>F) [9,15] to generate methylene-H<sub>4</sub>F directly, which is the C<sub>1</sub> donor for assimilation via the serine cycle. The second module is initiated by an enzyme-catalyzed reaction [9] of formaldehyde with a folate compound found

Received July 19, 2004; Accepted November 11, 2004; Published January 4, 2005

DOI: 10.1371/journal.pbio.0030016

Copyright: © 2005 Marx et al. This is an open-access article distributed under the terms of the Creative Commons Attribution License, which permits unrestricted use, distribution, and reproduction in any medium, provided the original work is properly cited.

Abbreviations: GC-MS, gas chromatography–mass spectrometry; H<sub>4</sub>F, tetrahydrofolate; H<sub>4</sub>MPT, tetrahydromethanopterin

Academic Editor: Rowena G. Matthews, University of Michigan, United States of America

\*To whom correspondence should be addressed. E-mail: lidstrom@u.washington.edu

‡Current address: Department of Microbiology and Molecular Genetics, Michigan State University, East Lansing, Michigan, United States of America

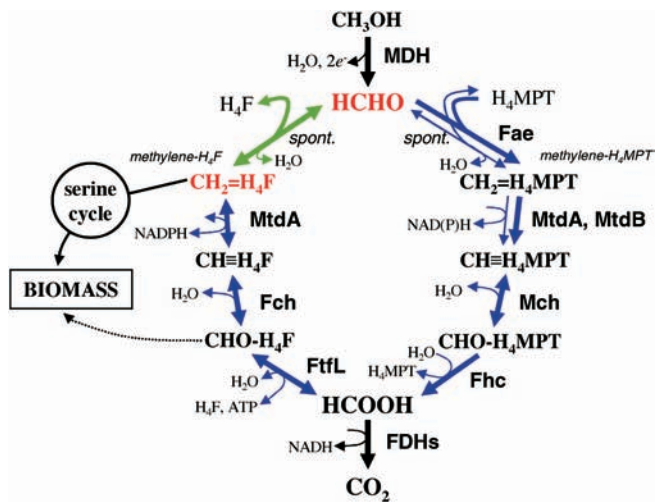


**Figure 1.** Formaldehyde Metabolism of *M. extorquens* AM1

Three modules work to provide two cellular outputs: formaldehyde assimilation and dissimilation. The direct condensation of formaldehyde with  $H_4F$  is shown in green. A second proposed route for generating methylene-tetrahydrofolate (methylene- $H_4F$ ), the consecutive action of the  $H_4MPT$  and  $H_4F$  modules is shown in blue. Fae, formaldehyde activating enzyme; Fch, methenyl  $H_4F$  cyclohydrolase; FDH, formate dehydrogenase; Fhc, formyltransferase/hydrolase complex; FftL, formyl  $H_4F$  ligase;  $H_4MPT$ , tetrahydromethanopterin; Mch, methenyl  $H_4MPT$  cyclohydrolase; MDH, methanol dehydrogenase; MtdA, methylene  $H_4F/H_4MPT$  dehydrogenase; MtdB, methylene  $H_4MPT$  dehydrogenase. Spontaneous and reversible reactions are indicated.

DOI: 10.1371/journal.pbio.0030016.g001

in methanogenic Archaea, tetrahydromethanopterin ( $H_4MPT$ ). The resulting methylene- $H_4MPT$  is subsequently oxidized through a series of reactions to formate [8,16,17], which can ultimately be dissimilated to  $CO_2$  via the activity of multiple formate dehydrogenases [18]. Finally, a third module involves interconversion of methylene- $H_4F$  and formate via a familiar set of  $H_4F$ -dependent reactions found in most organisms [11,19,20]. Mutant analysis has shown that both the  $H_4MPT$  and  $H_4F$  modules are required for growth on  $C_1$  compounds [8,9,10,11,12,13,19].

Two distinct models exist to explain the necessity of both the  $H_4MPT$  and  $H_4F$  modules in methylootrophy, predicting opposite directions for the net flux through the  $H_4F$  module. It was suggested over 20 y ago that the  $H_4F$  module functions in formaldehyde oxidation [21]. This predicts that the  $H_4MPT$  and  $H_4F$  modules are parallel, redundant formaldehyde oxidation systems. Recent genetic and biochemical evidence [11,12,13], however, suggest that the  $H_4F$  module is not functionally redundant to the  $H_4MPT$  module for formaldehyde oxidation. An alternative hypothesis suggests that the  $H_4F$  module functions in the reductive direction, generating methylene- $H_4F$  from formate [11,16,17]. This model suggests a single dissimilatory module ( $H_4MPT$  module) and two, redundant assimilatory modules: the  $H_4F$  module and the direct condensation of methylene- $H_4F$  from formaldehyde (Figure 1, green arrows). This model predicts two routes for generating the key assimilatory intermediate methylene  $H_4F$  from formaldehyde: one we will term “direct,” involving the direct condensation step, and one we will term “long,” involving the consecutive action of the  $H_4MPT$  and  $H_4F$  modules. Although the direct route (Figure

1, green arrows) requires flux through a nonenzymatic reaction, assimilation via the proposed long route (Figure 1, blue arrows) involving the action of the  $H_4MPT$  and  $H_4F$  modules is energetically costly due to a net expenditure of one ATP per  $C_1$  unit. If this hypothesis is correct, the  $H_4MPT$  module would play a role in both dissimilatory and assimilatory metabolism, in much the same way that the tricarboxylic acid cycle plays a dual role in growth on multicarbon compounds.

Clearly, this is an example in which metabolic reconstruction is not sufficient to predict the roles of the central metabolic modules involved in carbon partitioning. In addition, it provides a test case for how cells cope with a high-flux toxic metabolic intermediate. In order to address this problem, we have used a combination of stable isotope- and radioisotope-labeling approaches, which has allowed the complete determination of flux through every branch of methylootrophy. The results provide a dynamic picture of the response of *M. extorquens* AM1 during transitions in and out of methylootrophy. Furthermore, a kinetic model of the key formaldehyde utilization systems was developed that successfully predicted key system dynamics. Our data resolve the specific roles for three interconnected metabolic modules that have two cellular outputs, assimilation and dissimilation. Furthermore, we have revealed a new paradigm for handling high-flux toxic intermediates: a dynamic metabolic loop that demonstrates graded response to changing metabolic needs.

## Results

### Detection of Serine-Derived Mass Fragments Using Gas Chromatography–Mass Spectrometry

A  $CD_3OD$  label tracing strategy (Figure 2) was devised to directly determine what fraction of the methylene- $H_4F$  that entered the serine cycle was formed from the direct condensation of formaldehyde and  $H_4F$  (direct route), versus the fraction formed through the alternative potential route involving oxidation of formaldehyde to formate by the  $H_4MPT$  module, followed by assimilation through the  $H_4F$  module (long route). The serine that is produced from methanol contains the carbon atom, and both hydrogens, from the methylene group of the methylene- $H_4F$  donor. Serine produced from  $CD_3OD$  via the direct route contains two D, while that produced via the long route contains one D and in both cases these are relatively nonexchangeable C–D bonds. Therefore, at short labeling times (<1 min) the ratio of serine isotopomers with one or two D is an assay of the ratio of flux through the two routes.

In order for this label tracing method to be successful, the ratio of serine isotopomers containing one or two deuteriums from  $CD_3OD$  must be determined. Initially, cultures were labeled with standard methanol ( $CH_3OH$ ), added to boiling ethanol after labeling, and the derivatized  $H_2O$ -soluble small molecules were prepared and analyzed via gas chromatography–mass spectrometry (GC–MS). Consistent with a derivatized serine standard and previous work [22,23], a peak was observed at approximately 8.6 min that contained two major ions with  $M/z$  of 156 and 228 (Figure 2B and 2C). The proportion of (+1) and (+2)  $M/z$  ions detected were within  $1.1\% \pm 1.7\%$  and  $-0.7\% \pm 0.5\%$  of the predicted distribution (Isoform 1.02, National Institute of Standards and Technology) of naturally occurring heavy isotopomers for these

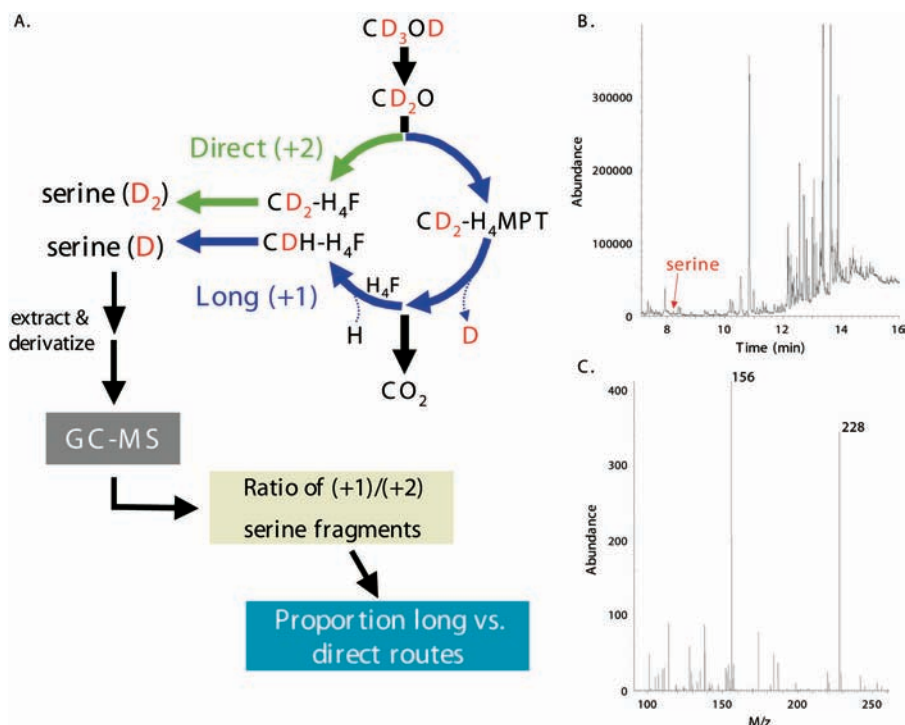


**Figure 2.** GC-MS Method to Assay Ratio of Long Versus Direct Routes

(A) Simplified model of formaldehyde metabolism highlighting the deuterium (in red) label-tracing strategy. Oxidation of deuterated methanol ( $\text{CD}_3\text{OD}$ ) leads to the production of formaldehyde with two deuteriums ( $\text{CD}_2\text{O}$ ). Direct condensation with  $\text{H}_4\text{F}$  (green arrows) and conversion to serine via the serine cycle (Figure 1) generates serine with two deuteriums. Alternatively, methylene- $\text{H}_4\text{F}$  may be produced through the long route (blue arrows; Figure 1), generating serine containing only one of the original deuteriums. Extraction and derivatization of small molecules for analysis by GC-MS provides the ratio of (+1)/(+2) serine isotopomers, thereby assaying the proportion of methylene- $\text{H}_4\text{F}$  generated via the long route through formate or from the direct route from formaldehyde.

(B) Detection of serine by GC-MS. The small peak in total ion abundance detected by the MS denoted by the arrow represents serine.

(C) Analysis of the mass fragments present in this peak revealed the presence of ions with  $M/z$  values of 156 and 228, which are diagnostic for ECF-TFAA derivatized serine.

DOI: 10.1371/journal.pbio.0030016.g002

fragments, indicating the feasibility of this GC-MS method for detecting serine isotopomers.

### Deuterium Labeling Demonstrates Assimilation of $\text{C}_1$ Units through Both Direct and Long Routes

Initially, the incorporation of deuteriums from  $\text{CD}_3\text{OD}$  into serine was investigated with succinate-grown cell suspensions of wild-type *M. extorquens* AM1. Analysis of the derivatized  $\text{H}_2\text{O}$ -soluble small molecule preparation from wild-type samples indicated a substantial increase in the proportion of fragments present as (+1) and (+2) isotopomers (>35% of total serine isotopomers).  $\text{CD}_3\text{OD}$  labeling with a *glyA* mutant strain (CM239K.1), which lacks the initial serine-cycle enzyme, serine hydroxymethyltransferase, and was therefore completely unable to assimilate carbon from formaldehyde, produced no increase in (+1) or (+2) isotopomers (data not shown). Additionally, mutants defective for the proposed long route for methylene- $\text{H}_4\text{F}$  formation were tested for deuterium labeling. These included the *fftL* (encodes formate- $\text{H}_4\text{F}$  ligase) mutant CM216K.1 [11], blocked for the  $\text{H}_4\text{F}$  module, and the *dmrA* (encodes dihydromethanopterin reductase) mutant CM212K.1 [24], which has been shown to lack  $\text{H}_4\text{MPT}$  [25,26]. Consistent with their proposed roles, the proportion of (+1) fragments dropped 8-fold for these mutants, compared to a modest 2-fold decrease in (+2) fragments. These data indicate that both the  $\text{H}_4\text{F}$  and  $\text{H}_4\text{MPT}$  modules affect labeling

of serine and are required to generate the large increase in (+1) isotopomers seen with wild-type. These data also indicate that potential exchange reactions that could eliminate the deuteriums do not contribute measurably to the presence of (+1) ions. Collectively, these data indicate that the (+1) and (+2) serine mass fragments can serve as an accurate proxy for methylene- $\text{H}_4\text{F}$  generated through the long or direct routes. One caveat to this statement is that a portion of the NADPH involved in generating methylene  $\text{H}_4\text{MPT}$  could be derived from the oxidation of methylene  $\text{H}_4\text{MPT}$  to methenyl  $\text{H}_4\text{MPT}$  and, therefore, could have become deuterium labeled. Based on the stoichiometry of the reactions and the known activity ratio of NADPH- versus NADH-producing enzymes for the methylene- $\text{H}_4\text{MPT}$  dehydrogenase reaction, we calculated that we at most overestimate the contribution of the direct pathway by 25% during growth on methanol, and by significantly smaller values at times with lower formaldehyde production. This prediction assumes an infinitely small intracellular concentration of NADPH, so depending on the actual pool of NADPH present, the error will be less. Therefore, our results are presented as maximum ratio changes.

When labeled with  $\text{CD}_3\text{OD}$ , the succinate-grown wild-type cultures utilized to verify the GC-MS method produced a ratio of (+1) versus (+2) serine mass fragments of  $8.0 \pm 0.6$ . Thus, when succinate-grown cells are first exposed to

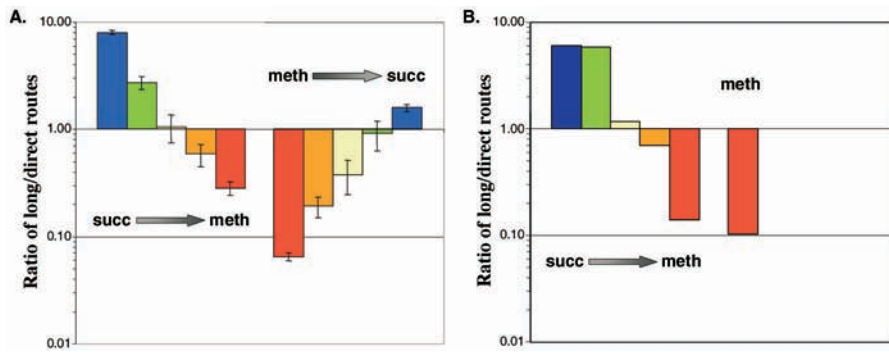


**Figure 3.** Change in Ratio of Flux through Long Versus Direct Methylene-H<sub>4</sub>F Formation Routes during Growth Transitions

(A) Experimental data as determined by GC-MS analysis of serine isotopomers. The bars for each transition represent a time series from cells harvested 1 h prior to the transition, and four time points following the transition (succinate to methanol: 1, 3, 5, and 7 h; methanol to succinate: 1, 3, 5, and 7 h).

(B) Predictions based on kinetic model simulations. The bars indicate the succinate to methanol transition (same time points as for the experimental data) and the methanol steady-state prediction.

DOI: 10.1371/journal.pbio.0030016.g003

methanol, the majority of methylene-H<sub>4</sub>F assimilated via the serine cycle is generated via the proposed long route. In contrast, CD<sub>3</sub>OD labeling of mid-exponential-phase methanol-grown cells indicated that the direct route dominated by up to 15-fold (measured ratio of [+1]/[+2] of  $0.065 \pm 0.006$ ). Therefore, although both methylene-H<sub>4</sub>F production routes operated under both physiological conditions, a significant shift in the ratio of the two routes occurred, up to 100-fold.

#### Relative Contributions of the Long and Direct Routes of Methylene-H<sub>4</sub>F Formation during Transitions to and from Methylo-trophic Growth

In order to understand the dynamics of the contribution of the long and direct routes for directing C<sub>1</sub> units into

assimilatory metabolism during transitions to and from methylo-trophic growth, metabolic shift experiments were performed. One hour after samples were removed from succinate- and methanol-grown cultures for the labeling experiments described above, the remaining portions of the two cultures were harvested, washed, and resuspended into medium containing the other substrate (methanol or succinate, respectively). At four intervals during the transition to each of the new growth substrates (Figure 3) samples were harvested and analyzed via CD<sub>3</sub>OD labeling to determine the ratio of flux capacity through the two methylene-H<sub>4</sub>F formation routes. The ratio of the contribution of the long route for methylene-H<sub>4</sub>F formation to the direct route varied in a continuous fashion during the transition from succinate

**Table 1.** Calculated C<sub>1</sub> Fluxes during Transitions between Succinate and Methanol at the Time (h) Relative to the Transition

Transition	Branch	Flux				
		-1	1	5/3 <sup>a</sup>	7.5/5 <sup>a</sup>	10/7 <sup>a</sup>
Succinate to methanol	A	1.9 ± 0.1	3.7 ± 0.1	13.2 ± 1.0	14.5 ± 1.0	19.2 ± 0.2
	B	1.9 ± 0.1	3.6 ± 0.1	11.4 ± 0.8	11.8 ± 0.9	15.3 ± 0.2
	C	1.6 ± 0.1	3.3 ± 0.1	9.7 ± 1.2	10.3 ± 1.0	14.2 ± 0.2
	D	1.6 ± 0.1	3.1 ± 0.1	8.6 ± 1.2	8.9 ± 1.0	12.6 ± 0.2
	E	0.2 ± <0.1	0.4 ± <0.1	1.7 ± 0.4	1.5 ± 0.2	1.1 ± 0.1
	F	<0.1 ± <0.1	0.1 ± <0.1	1.7 ± 0.2	2.7 ± 0.2	3.9 ± 0.2
	G	0.2 ± <0.1	0.5 ± <0.1	3.5 ± 0.2	4.3 ± <0.1	5.0 ± 0.1
	H	0.1 ± <0.1	0.2 ± <0.1	1.1 ± <0.1	1.3 ± <0.1	1.6 ± <0.1
	I	<0.1 ± <0.1	0.1 ± <0.1	0.6 ± <0.1	0.8 ± <0.1	0.9 ± <0.1
	J	0.3 ± <0.1	0.7 ± <0.1	5.2 ± 0.2	6.4 ± <0.1	7.5 ± 0.2
Methanol to succinate	A	20.6 ± 1.0	10.2 ± 1.3	9.1 ± 0.6	7.5 ± 0.4	4.8 ± 0.3
	B	13.9 ± 0.9	6.4 ± 0.7	6.4 ± 0.8	5.8 ± 0.6	4.3 ± 0.3
	C	13.5 ± 0.9	5.6 ± 0.6	5.5 ± 0.5	4.4 ± 0.5	3.5 ± 0.3
	D	11.3 ± 0.9	4.2 ± 0.4	4.3 ± 0.5	3.5 ± 0.5	3.1 ± 0.3
	E	0.4 ± <0.1	0.7 ± 0.1	1.0 ± 0.3	1.4 ± 0.2	0.8 ± <0.1
	F	6.6 ± 0.1	3.9 ± 0.7	2.7 ± 0.3	1.7 ± 0.2	0.5 ± <0.1
	G	7.0 ± 0.1	4.6 ± 0.7	3.7 ± 0.1	3.0 ± 0.1	1.3 ± 0.1
	H	2.2 ± <0.1	1.5 ± 0.2	1.2 ± <0.1	1.0 ± <0.1	0.4 ± <0.1
	I	1.3 ± <0.1	0.8 ± 0.1	0.7 ± <0.1	0.6 ± <0.1	0.2 ± <0.1
	J	10.6 ± 0.2	6.9 ± 1.1	5.5 ± 0.1	4.6 ± 0.1	1.9 ± 0.1

All values are reported in nmol, min<sup>-1</sup>, mL<sup>-1</sup>, and OD<sub>600</sub><sup>-1</sup>.

<sup>a</sup> First number represents flux for succinate to methanol; second number represents flux for methanol to succinate.

DOI: 10.1371/journal.pbio.0030016.t001

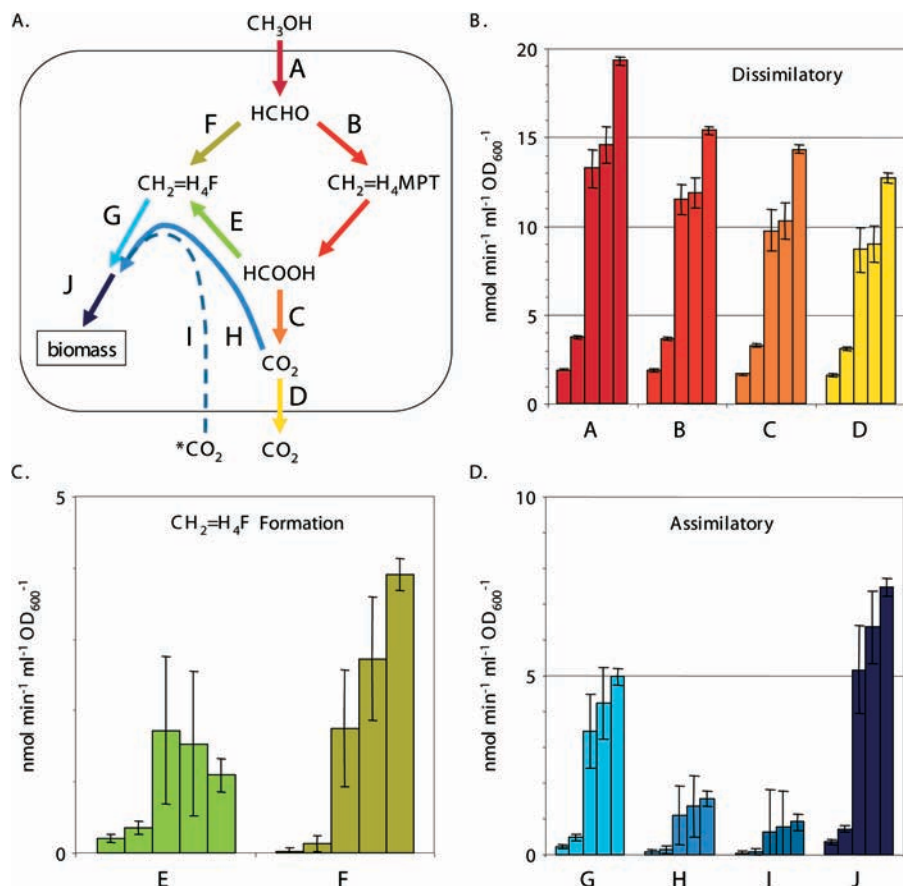


**Figure 4.** C<sub>1</sub> Fluxes during Transition from Succinate to Methanol

The fluxes determined are represented schematically (A). The other panels present flux for each branch, labeled A through J. The five bars for each flux represent a time series from cells harvested 1 h prior to the transition from succinate to methanol, and 1, 5, 7.5, and 10 h after the switch. Dissimilatory (B), methylene-H<sub>4</sub>F formation (C), and assimilatory (D) fluxes are presented separately with different scales for clarity. Flux F represents maximum fluxes.

DOI: 10.1371/journal.pbio.0030016.g004

to methanol, or from methanol to succinate (Figure 3A). The cultures were followed for 7 or 10 h after the shift—sufficient time to observe the majority of the transition.

#### Dynamics of C<sub>1</sub> Fluxes during Transitions between Succinate and Methanol by <sup>14</sup>C Labeling

The relative ratio of the routes provides only one of the parameters needed to understand the metabolic dynamics during this transition; the quantitative flux is also necessary. These values were obtained with <sup>14</sup>C-labeling experiments. Concurrent with the CD<sub>3</sub>OD-labeling experiments described above, a portion of each sample was used to determine the rates of methanol oxidation, assimilation of C<sub>1</sub> units, and CO<sub>2</sub> production via <sup>14</sup>C-CH<sub>3</sub>OH labeling [11]. Methanol oxidation was found to be 10-fold higher in methanol-grown cultures, and the percentage of carbon from methanol assimilated into biomass was 3-fold higher as compared to succinate-grown cultures (Table 1). The other values incorporated into the flux calculations are the stoichiometry of the serine cycle, in which two C<sub>1</sub> units from methylene-H<sub>4</sub>F and one CO<sub>2</sub> are incorporated for every C<sub>3</sub> compound assimilated, and the proportion of external, unlabeled CO<sub>2</sub> incorporated by the serine cycle [27]. The ten C<sub>1</sub> fluxes (each branch arbitrarily labeled “A” through “J”) calculated using the concurrent

CD<sub>3</sub>OD and <sup>14</sup>C-methanol labeling methods are reported in Table 1 and shown in Figures 4 and 5.

A comparison of the values for succinate- versus methanol-grown cells shows that upon initial exposure of succinate-grown cells to methanol (Figure 4 and Table 1), the measurements suggest that most (at least 99%) of the formaldehyde was handled by the H<sub>4</sub>MPT module (flux B), and only a small amount flowed through the direct route (flux F). Of formate made from the H<sub>4</sub>MPT module (flux B), most (up to 88%) was converted to CO<sub>2</sub> via formate oxidation (flux C), and a smaller amount (at least 12%) flowed through the H<sub>4</sub>F module and into assimilation (flux E), representing at least 90% of the assimilatory carbon. In contrast, for methanol-grown cells (Figure 5 and Table 1), less (only about 70%) of the formaldehyde generated from methanol flowed through the H<sub>4</sub>MPT module (flux B), with up to 30% handled by the direct route (flux F). Only a small portion of the assimilatory carbon (suggested to be about 6%) flowed through the H<sub>4</sub>F module (flux E), which represented about 3% of the formate generated via the H<sub>4</sub>MPT module. The remainder of the formate was oxidized to CO<sub>2</sub> (flux C). These data indicate that, although the relative contribution of the long route to methylene-H<sub>4</sub>F formation decreased during the transition to growth on methanol (see Figure 3), the flux

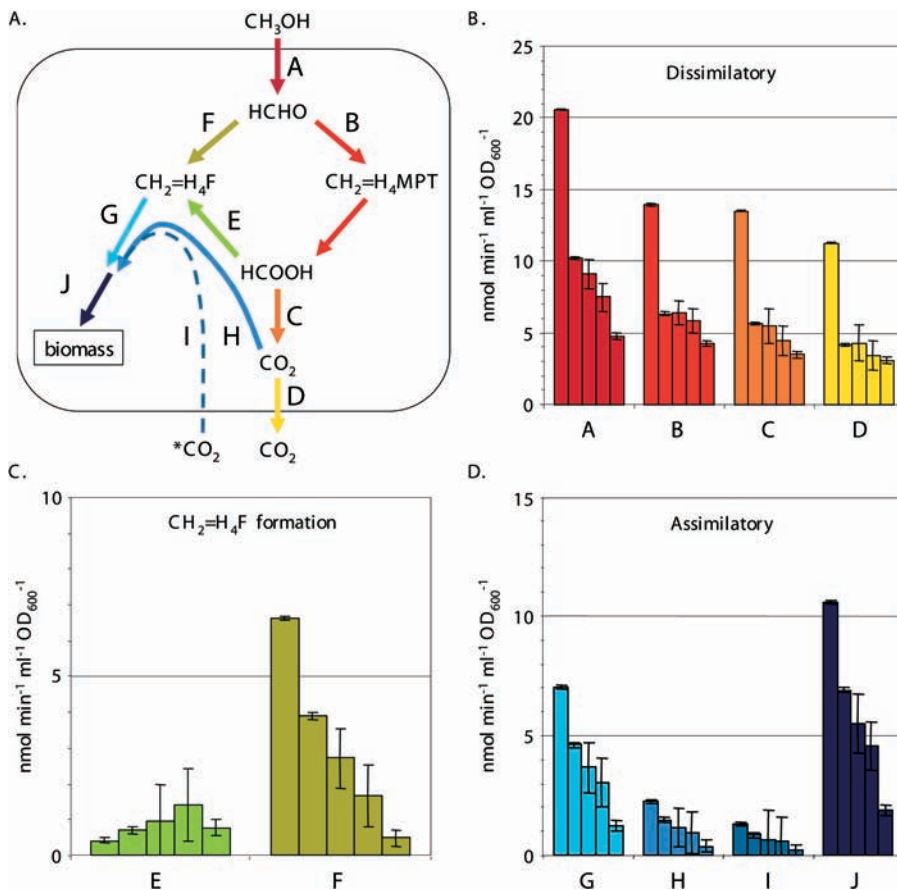


**Figure 5. C<sub>1</sub> Fluxes during Transition from Methanol to Succinate**

The fluxes determined are represented schematically (A). The other panels present flux for each branch, labeled A through J. The five bars for each flux represent a time series from cells harvested 1 h prior to the transition from methanol to succinate, and 1, 3, 5, and 7 h after the switch. Dissimilatory (B), methylene-H<sub>4</sub>F formation (C), and assimilatory (D) fluxes are presented separately with different scales for clarity. Flux F represents maximum fluxes.

DOI: 10.1371/journal.pbio.0030016.g005

through the long route (flux E) increased significantly (see Figure 4). Flux through this route peaked 5 h after the transition to methanol, when it reached a value at least 8-fold higher than succinate-grown cells, and dropped somewhat

afterward. The flux through the direct route (flux F) also increased to a maximum of up to 20% of the total formaldehyde flux at the final time point during the transition (see Figure 4). The fluxes for the transition from

**Table 2. Equilibrium Constants and Forward Rate Constants ( $V_{max}$ ) for Each Reaction in the Model Simulation**

Reaction Number	Reaction Enzyme	$K_{eq}$	$V_i$ (Methanol)	$V_i$ (Succinate)	Source
1	Formaldehyde-activating enzyme	Irrev.	78.0	16.71	[9]
2a	Me-H <sub>4</sub> MPT dehydrogenase (MtdB)	174.2	10.5	2.1	[8]
2b	Me-H <sub>4</sub> MPT dehydrogenase (MtdA)	174.2	2.42	2.42	[38]
3	Mn-H <sub>4</sub> MPT cyclohydrolase	0.137	4.62	1.54	[20]
4	Formyltransferase	0.204	0.96	0.96	[17] <sup>a</sup>
5	Formylhydrolase	Irrev.	16.21	16.21	Fitted
6	Nonenzymatic	NA	2.64	2.64	Fitted
7	Me-H <sub>4</sub> F dehydrogenase (MtdA)	0.249	0.71	0.172	[38]
8	Mn-H <sub>4</sub> F cyclohydrolase	10.6	2.27	0.75	[20]
9	Formyl-H <sub>4</sub> F ligase	0.0418	2.76 (s <sup>-1</sup> )	2.76 (s <sup>-1</sup> )	Fitted
10	Formate dehydrogenase	Irrev.	1.049	0.1776	[18] <sup>b</sup>
11	Serine hydroxymethyltransferase	NA	20.0	3.116	Fitted

Equilibrium constants are all dimensionless, except for reaction 9, which has units of mM. Units for kinetic constants are mM/sec unless otherwise noted.

<sup>a</sup> The literature value for this constant is 0.71 mM/s. A small adjustment was required to fit the data.

<sup>b</sup> Constants of twice the literature values were assumed, due to the presence of multiple formate dehydrogenases.

H<sub>4</sub>F, tetrahydrofolate; H<sub>4</sub>MPT, tetrahydromethanopterin; me-H<sub>4</sub>F, methylene-H<sub>4</sub>F; me-H<sub>4</sub>MPT, methylene-H<sub>4</sub>MPT; MFR, methanofuran; mn-H<sub>4</sub>F, methenyl-H<sub>4</sub>F; mn-H<sub>4</sub>MPT, methenyl-H<sub>4</sub>MPT; Irrev., irreversible; NA, not applicable.

DOI: 10.1371/journal.pbio.0030016.t002

methanol to succinate represent the capacity for flux, as no methanol was present after the growth transitions. These changes, however, roughly mirrored the transition from succinate to methanol, but were not an exact reversal (see Figure 5). As noted for the deuterium-labeling experiments, the time periods followed in these experiments were sufficient to observe the majority of the transition.

### Dynamic Mathematical Model of Formaldehyde Partitioning

In order to assess whether the known kinetic constraints of the three modules of formaldehyde metabolism were sufficient to account for the experimentally determined flux dynamics, a mathematical model was generated. The model simulated partitioning of  $C_1$  units through the three formaldehyde modules during growth of cells in methanol, and for the transition of succinate-grown cells to methanol. The model consisted of eight ordinary differential equations, based on known kinetic mechanisms, to describe the dynamics of the  $H_4F$  and  $H_4MPT$  modules and the direct condensation reaction. Most binding constants, rate constants, and cofactor concentrations were obtained from the literature (Table 2). For the six cases in which literature values are not known, these were estimated as described in Materials and Methods. Additionally, a dynamic simulation of the succinate to methanol transition was performed. The methanol uptake rate was set to the experimentally measured value at each time point (flux A, Table 1) and interpolated linearly between time points to create a smooth gradient. Starting with the values obtained for succinate or methanol growth, the parameters were increased throughout the shift at a rate corresponding to the increase in methanol uptake.

Two key results are apparent from the comparison of the model's predictions (see Figure 3B) to the measured flux ratio of the two methylene- $H_4F$  production routes (see Figure 3A). First, the model did not constrain the direction of flux through the  $H_4F$  module. Therefore the prediction that the  $H_4F$  module functions in assimilation both during steady-state methanol growth and upon the first exposure of succinate-grown cells to methanol indicates that the kinetic parameters of the module components are sufficient to account for this phenomenon. Second, the correspondence between the predicted and experimentally determined dynamics of the switch in methylene- $H_4F$  production routes confirms that the dynamics of the system are also largely attributable to the systems' kinetic constraints. That the kinetics did not exactly mimic the measured values is presumably partly due to differences between the actual induction of enzyme activities versus the model's simplifying assumption that all values change in a manner directly proportional to changes in methanol uptake. However, the model does not suggest a significant effect of methylene  $H_4MPT$ -derived NADPD in the deuterium-labeling studies.

### The $H_4F$ Module Could Not Be Eliminated during Growth on $C_1$ Compounds

The combination of  $CD_3OD$  and  $^{14}C$ -methanol label-tracing studies clearly demonstrate that the long route contributes methylene- $H_4F$  to the serine cycle and that the flux through the  $H_4F$  module portion of the long route (flux E) increases significantly during the transition to growth on methanol. These results confirm the hypothesis of net

reductive flux through this module [11,16,17]. However, this route contributes only 6% of the total methylene- $H_4F$  generated during growth on methanol. Therefore, it seemed possible that the  $H_4F$  module might be required during transitions in and out of methylotrophy, but might not be required for continuous growth on methanol. Given the available genetic techniques, two strategies were employed in an attempt to obtain mutants in one of the key  $H_4F$  module genes, formate- $H_4F$  ligase, during growth on  $C_1$  compounds. First, attempts were made to obtain null mutants via allelic exchange with cultures maintained on methanol or methylamine, but these efforts were unsuccessful. Second, cultures of the *ΔftfL::kan* mutant CM216K.1 [11] bearing the complementing plasmid pCM218 [11] were grown in medium containing methanol or methylamine without tetracycline for plasmid maintenance. No plasmid-free isolates were obtained for CM216K.1 with pCM218 during growth on methanol. However, they were obtained for wild-type with pCM218 on methanol, or CM216K.1 with pCM218 grown on succinate. Therefore, it appears that the  $H_4F$  module plays an essential role in methylotrophy even after cells have already begun to grow on  $C_1$  compounds.

## Discussion

In the formaldehyde metabolism of *M. extorquens* AM1, three interconnected metabolic modules are present, involved in two roles: converting formaldehyde to the key assimilatory intermediate methylene  $H_4F$  and net oxidation of formaldehyde to  $CO_2$ . Understanding paradigms for differential roles of redundant modules is central to enabling broadscale metabolic reconstruction from genome sequences. In addition, methylotrophy represents an intriguing example of a metabolic mode in which growth depends on high flux of a toxic metabolite, with subsequent partitioning of that metabolite. Other such modes are known that produce toxic aldehydes, for instance, growth on ethanolamine [28] and other alcohols [29]. Numerous other toxic intermediates are known in bacteria, such as the production of hydroxylamine by ammonia-oxidizing bacteria [30] and mono-oxygenase-dependent production of epoxyalkanes during growth on aliphatic alkanes [31]. In addition, the liver can be exposed to toxic metabolites, for instance, the production of formate from acute methanol poisoning [32]. However, the metabolic mechanisms that allow the balancing of flux and toxicity in such situations are not well understood. Understanding paradigms for such metabolic responses is important for assessing and possibly ameliorating toxicity problems in a variety of systems, including bioremediation of toxic compounds, chemical production in bioprocesses, and detoxification in tissues and organs.

Through a combination of  $^{14}C$  and deuterium label-tracing strategies, we have defined flux through each metabolic module in methylotrophic metabolism in *M. extorquens* AM1 during transitions into and out of methylotrophy, in which the flux of formaldehyde into the system changed by a factor of 10. These methods had the dual advantages of possessing sufficient sensitivity to detect flux under all conditions tested, and being free from the requirement of steady-state growth conditions, which allowed the dynamics of growth transitions to be examined. Furthermore, this approach complements a recently developed  $^{13}C$ -labeling method that measures flux

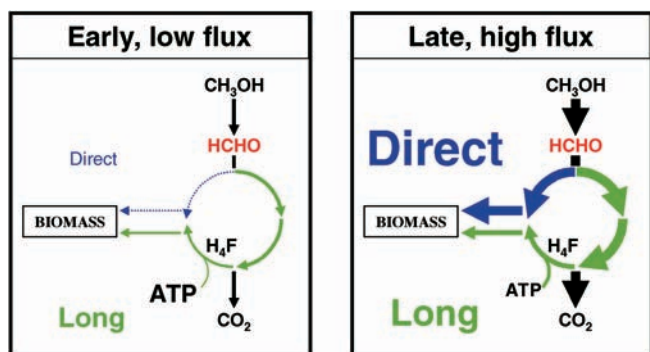


**Figure 6.** An Interconnected Metabolic Loop for Handling the Toxic Intermediate Formaldehyde

A dynamic transition occurs from low to high formaldehyde flux, shifting the ratio of the direct versus long routes, and in the relative proportion of carbon oxidized to  $\text{CO}_2$  versus assimilated, creating a buffer system to accommodate large changes in formaldehyde flux. DOI: 10.1371/journal.pbio.0030016.g006

through the multicarbon branches of central metabolism [27], but is inherently silent to the  $\text{C}_1$  fluxes measured here. The approach described here allowed us to test and confirm the hypothesis that the role of the  $\text{H}_4\text{F}$  module during growth on  $\text{C}_1$  compounds is to supply methylene- $\text{H}_4\text{F}$  from formate [11,16,17], although the fraction of total flux passing through this route is always small.

Given the small percentage of total flux into assimilation via the  $\text{H}_4\text{F}$  module during growth on methanol, why is this module required under this condition? The results presented here suggest that this requirement is not alleviated even when cells begin to actively grow on methanol. It is possible that this module generates an inducing signal for the serine cycle and, therefore, is necessary to maintain assimilatory flux during growth on methanol. This hypothesis is consistent with the genetic circuit, as two of the genes encoding key enzymes of the  $\text{H}_4\text{F}$  module (*mtdA* and *fch*) are in an operon with serine-cycle genes and are under the control of a single regulatory protein, QscR [33].

Our results demonstrate a dramatic shift in flux through the primary methylotrophic modules during these transitions. It has long been known that all enzymes of methylotrophy increase 3–6 fold in activity after induction with methanol [14,16], predicting a sizable increase in total flux into the system. However, the flux measurements reported here show that a dynamic repartitioning occurs also. When *M. extorquens* AM1 encounters methanol, the methanol oxidation system is at low but significant activity [34]. Under these conditions, the flux of formaldehyde into the system is relatively low (Figure 6, left panel), and most of the formaldehyde is oxidized to  $\text{CO}_2$  via the  $\text{H}_4\text{MPT}$  module and formate dehydrogenase, generating NAD(P)H. Only a trace amount is assimilated, almost all of that through the long route involving formate and  $\text{H}_4\text{F}$  intermediates. As the flux of formaldehyde into the system increases, a greater percentage begins to flow through the direct route into assimilatory metabolism. A smooth transition occurs during the induction of the capacity in the system until approximately one-third of the total formaldehyde flows through this route, and assimilatory and dissimilatory metabolism are balanced for rapid growth on methanol (Figure 6, right

panel). The metabolic elegance of this interconnected, dynamic metabolic loop creates an effective formaldehyde flux buffer for transitions, in which the cell has time to respond to the presence of a methylotrophic substrate, deriving benefit (energy) without risking buildup of a toxic intermediate. As the activity of the serine cycle begins to increase, more formaldehyde can be safely shunted to assimilatory metabolism via the direct, ATP-independent route, thereby ensuring the transition to growth on the  $\text{C}_1$  substrate without build up of formaldehyde.

What controls the rate of the nonenzymatic condensation of formaldehyde with  $\text{H}_4\text{F}$  to form methylene- $\text{H}_4\text{F}$ , which was up to 150-fold greater during methanol growth than on succinate? The rate of this spontaneous reaction will be determined by the relative concentrations of reactants and products, with an equilibrium constant for this condensation of  $3.2 \times 10^{-4}$  [15]. Although this equilibrium constant favors the production of methylene- $\text{H}_4\text{F}$ , flux will only occur if either the concentrations of the reactants (formaldehyde and/or  $\text{H}_4\text{F}$ ) rise above the equilibrium concentration, or utilization of methylene- $\text{H}_4\text{F}$  is sufficient to keep the pool of this metabolite below the equilibrium concentration. At this time, it is not technically feasible to measure the intracellular concentrations of free formaldehyde or methylene- $\text{H}_4\text{F}$ . However, the most likely explanation for high flux through the nonenzymatic condensation of formaldehyde and  $\text{H}_4\text{F}$  would be draw-off of the product (methylene- $\text{H}_4\text{F}$ ) by the serine cycle. In order to test whether the known kinetic parameters explain the relative utilization of the two methylene- $\text{H}_4\text{F}$  production routes, a kinetic model was constructed and utilized to simulate formaldehyde partitioning during transitions to and from methylotrophic growth. The ability of the model to recapitulate the observed switch in route utilization (see Figure 3B) indicates that the architecture of the dynamic loop and the kinetic parameters of the responsible enzymes can predict operation of the  $\text{H}_4\text{F}$  module in the assimilatory direction and are sufficient to account for partitioning of  $\text{C}_1$  units into assimilatory metabolism without accumulation of formaldehyde.

In summary, the dual-labeling approach described here for direct flux measurement during metabolic transitions has not only elucidated a key role for redundancy in the three metabolic modules responsible for formaldehyde assimilation and dissimilation, but has also revealed a new paradigm for accommodating high-flux toxic intermediates. It is likely that similar interconnected loop systems operate for other metabolites, toxic or not, and this example can now be used as a framework for predicting functions of other apparently redundant modules that may be involved in the handling of toxic metabolites.

## Materials and Methods

**Bacterial strains.** Wild-type *M. extorquens* AM1 [35] and mutant strains were cultured at 30 °C in a minimal salts medium [36] containing 125 mM methanol or 15 mM succinate. A serine hydroxymethyltransferase mutant strain, CM239K.1 (*AglyA::kan*) was generated using the allelic exchange technique described previously [37].

**$\text{CD}_3\text{OD}$  labeling and GC-MS.**  $\text{CD}_3\text{OD}$  (99.8%; Cambridge Isotope Laboratories, Andover, Massachusetts, United States) to a final concentration of 1 mM was added to washed cultures that had been resuspended to an  $\text{OD}_{600} = 1$  in order to label cell metabolites with deuterium for analysis by GC-MS. After shaking for 20 s at room

temperature the 2-ml suspension was added to three volumes of boiling 100% ethanol for instant lysis. Following centrifugation, the soluble fraction was dried, resuspended in distilled H<sub>2</sub>O, and centrifuged again to remove H<sub>2</sub>O-insoluble components. The resulting H<sub>2</sub>O-soluble small molecule fraction was then derivatized with ethyl chloroformate and trifluoroacetic acid as previously described [22,23]. All labeling experiments were performed three times.

**GC-MS methods and data analysis.** GC-MS experiments were performed using an Agilent 6890 gas chromatograph/Agilent 5973 quadrupole mass selective detector (electron impact ionization) operated at 70 eV equipped with an Agilent 7683 autosampler/injector (Hewlett-Packard, Palo Alto, California, United States). The MS was operated in selected ion monitoring mode to detect  $M/z = 156/157/158/228/229/230$  from 7 min to the end of the method. The GC oven temperature started at an initial temperature of 60 °C, ramping at 20 °C min<sup>-1</sup> to 130 °C, 4 °C min<sup>-1</sup> to 155 °C, and then 120 °C min<sup>-1</sup> to a final temperature of 300 °C that was held for 5 min. Flow through the column was held constant at 1 ml min<sup>-1</sup>. The injection volume was 1 µl and the machine was run in splitless mode. The temperature of the inlet was 230 °C, the interface temperature was 270 °C, and the quadrupole temperature was 150 °C. The column utilized was an HP-5MS (Hewlett-Packard).

GC-MS data were analyzed using Agilent Enhanced ChemStation G1701CA (Hewlett-Packard). The two mass clusters for serine,  $M/z = 156/157/158$ , and  $228/229/230$ , represent fragments of ECF-TFAA derivatized serine (C<sub>10</sub>H<sub>14</sub>O<sub>6</sub>NF<sub>5</sub>) that have lost one or both of the carboxyl ethyl esters. The data were corrected for the natural abundance of heavy isotopes in the derivatized serine fragments, using proportions calculated with Isoform 1.02 (MS Search Program for Windows, National Institute of Standards and Technology, Gaithersburg, Maryland, United States). For each sample, the ratio of  $(\Delta + 1)/(\Delta + 2)$  was calculated for both mass clusters and averaged. The mean and standard error for these data were then calculated for the three replicates of each experiment.

**Assimilation and CO<sub>2</sub> production rates.** The rate of <sup>14</sup>C-CO<sub>2</sub> production and assimilation of labeled carbon from <sup>14</sup>C-methanol was determined concurrently with the CD<sub>3</sub>OD labeling described above using a modification of a previously described method [11]. A portion of the labeled cell suspensions was filtered (0.2 µM PVDF, Millipore, Billerica, Massachusetts, United States) to determine net assimilation. All measured and calculated fluxes were determined using the data from each of the three replicate experiments and then utilized to determine the mean and standard error for each flux.

**Additional values incorporated into flux calculations.** It has been determined previously that 63.3% of the total CO<sub>2</sub> incorporated originates directly from CO<sub>2</sub> produced from the oxidation of methanol [27]. This value cannot be determined under the nonsteady state conditions used in the experiments described here, so this value was incorporated directly into our calculations. The sensitivity of the calculated fluxes to a 2-fold increase or decrease in the determined ratio of 1.73:1.00 internal:external CO<sub>2</sub> incorporated into the serine cycle was examined. Besides the direct effect on relative fluxes of internal and external CO<sub>2</sub> into the serine cycle, the calculated incorporation of C<sub>1</sub> units from methylene-H<sub>4</sub>F would vary no more than 7%, which would be balanced by a change in the dissimilatory flux through the H<sub>4</sub>MPT module and formate dehydrogenase of less than 6%. Therefore, deviations in the ratio of methanol-derived and external CO<sub>2</sub> incorporation from the reported work [27] would not significantly alter the calculated fluxes.

**Dynamic model.** The dynamic model of the formaldehyde oxidation and assimilation modules consisted of eight ordinary differential equations, each describing the accumulation of a metabolite involved in the H<sub>4</sub>F and H<sub>4</sub>MPT modules. These equations were derived in a straightforward manner from the kinetic expressions given below. The production of formaldehyde from methanol was set to the measured rate of methanol uptake for each experiment. All enzymatic reactions were treated with either uni- or bimolecular reversible Michaelis-Menten kinetics, with the equilibrium constants taken from the literature [38]. In cases where  $K_{eq} > 200$ , the reverse reaction was ignored for simplicity. Finally, since the dynamics of serine and glycine were not included in this model, serine hydroxymethyltransferase was modeled as an irreversible unimolecular Michaelis-Menten reaction, with the effects of all metabolites other than methylene-H<sub>4</sub>F accounted for in an effective  $V_{max}$ . The total internal concentrations of H<sub>4</sub>F and H<sub>4</sub>MPT derivatives were set equal to 0.15 and 0.4 mM, respectively [38]. Concentrations of other energy and redox cofactors (ATP, NADH, etc.) were assumed equal to those present in *Escherichia coli* [39]. The parameters used in the simulation are listed in Table 2. All  $K_m$ s

could be obtained from the literature (see Table 2), except for that of reaction 5. This  $K_m$  was set arbitrarily to 50 µM, which results in the reaction proceeding at half-maximal rate. Many of the values for  $V_{max}$  could be directly calculated from specific activities found in the literature, for both growth on methanol and succinate. To allow for experimental error in the measured rate constants, and to account for the fact that kinetics measured in vitro do not necessarily correlate exactly with what occurs inside the cell, these values were allowed to vary within 50% during the fitting procedure described below. For the remaining parameters, a numerical error minimization technique was used to find the set of parameters yielding model predictions with the best fit to the experimental flux distributions, when integrated to steady state. This was first done for methanol growth, then repeated for succinate growth. The rate constant for spontaneous formaldehyde condensation ( $k_6$ ) was forced to be the same on succinate as on methanol, since this is a fundamental chemical property that is not affected by gene induction. All reverse rate constants were calculated directly from the forward constants, binding constants, and  $K_{eq}$ . The spontaneous condensation of formaldehyde with H<sub>4</sub>MPT was assumed to be negligible under physiological conditions compared to the formaldehyde activating enzyme reaction [9]. All simulations were performed in MATLAB 6.5 (MathWorks, Natick, Massachusetts, United States) using the ODE solving function "ode15s." The error minimization was also done in MATLAB, using an evolutionary algorithm written previously [27].

$$r_1 = V_6[\text{H4MPT}] + V_1 \left( \frac{[\text{H4MPT}]}{K_{m1a} + [\text{H4MPT}]} \right) \left( \frac{[\text{HCHO}]}{K_{m1b} + [\text{HCHO}]} \right)$$

$$r_{2a} = V_{2a} \left( \frac{[\text{me} - \text{H4MPT}]}{K_{m2a} + [\text{me} - \text{H4MPT}]} \right) \left( \frac{[\text{NAD}]}{K_{m2b} + [\text{NAD}]} \right)$$

$$r_{2b} = V_{2b} \left( \frac{[\text{me} - \text{H4MPT}]}{K_{m2a} + [\text{me} - \text{H4MPT}]} \right) \left( \frac{[\text{NADP}]}{K_{m2b} + [\text{NADP}]} \right)$$

$$r_3 = \frac{K_{m3r} V_3 [\text{mn} - \text{H4MPT}] - K_{m3} V_3^{rev} [\text{formyl} - \text{H4MPT}]}{K_{m3} K_{m3r} + K_{m3r} [\text{mn} - \text{H4MPT}] + K_{m3} [\text{formyl} - \text{H4MPT}]}$$

$$r_4 = \frac{V_4 \frac{[\text{formyl} - \text{H4MPT}][\text{MFR}]}{K_{m4a} K_{m4b}} - V_{4r} \frac{[\text{formyl} - \text{MFR}][\text{H4MPT}]}{K_{m4ar} K_{m4br}}}{\left( 1 + \frac{[\text{formyl} - \text{H4MPT}]}{K_{m4a}} + \frac{[\text{MFR}]}{K_{m4b}} \right) \left( 1 + \frac{[\text{formyl} - \text{MFR}]}{K_{m4ar}} + \frac{[\text{H4MPT}]}{K_{m4br}} \right)}$$

$$r_5 = V_5 \left( \frac{[\text{formyl} - \text{MFR}]}{K_{m5} + [\text{formyl} - \text{MFR}]} \right)$$

$$r_6 = V_6[\text{H4F}][\text{HCHO}]$$

$$r_7 = \frac{V_7 \frac{[\text{me} - \text{H4F}][\text{NADP}]}{K_{m7a} K_{m7b}} - V_{7r} \frac{[\text{mn} - \text{H4F}][\text{NADPH}]}{K_{m7ar} K_{m7br}}}{\left( 1 + \frac{[\text{me} - \text{H4F}]}{K_{m7a}} + \frac{[\text{NADP}]}{K_{m7b}} \right) \left( 1 + \frac{[\text{mn} - \text{H4F}]}{K_{m7ar}} + \frac{[\text{NADPH}]}{K_{m7br}} \right)}$$

$$r_8 = \frac{K_{m8r} V_8 [\text{mn} - \text{H4F}] - K_{m8} V_8^{rev} [\text{formyl} - \text{H4F}]}{K_{m8} K_{m8r} + K_{m8r} [\text{mn} - \text{H4F}] + K_{m8} [\text{formyl} - \text{H4F}]}$$

$$r_9 = V_9 [\text{formyl} - \text{H4F}] - V_9^{rev} \frac{[\text{ATP}]}{[\text{ADP}]} [\text{HCOOH}][\text{H4F}]$$

$$r_{10} = V_{10} \left( \frac{[\text{HCOOH}]}{K_{m10} + [\text{HCOOH}]} \right)$$

$$r_{11} = V'_{11} \left( \frac{[\text{me} - \text{H4F}]}{K_{m10} + [\text{me} - \text{H4F}]} \right)$$

Abbreviations as in Table 2.

## Supporting Information

### Accession Numbers

The GenBank (<http://www.ncbi.nlm.nih.gov/Genbank>) accession numbers for genes discussed in this paper are *dmrA* (AY093431), *fffL* (AY279316), and *glyA* (L33463).

### Acknowledgments

We would like to thank L. Chistoserdova, M. Kalyuzhnaya, N.

Korotkova, H. Rothfuss, S. Stolyar, R. Thauer, and J. Vorholt for their thoughtful discussion of our work, M. Sadilek for his invaluable assistance in developing the GC-MS method, and anonymous reviewers for helpful comments. This work was supported by a grant from the National Institutes of Health (GM 36296).

**Competing interests.** The authors have declared that no competing interests exist.

**Author contributions.** CJM, SJVD, and MEL conceived and designed the experiments. CJM and SJVD performed the experiments. CJM, SJVD, and MEL analyzed the data. CJM and SJVD contributed reagents/materials/analysis tools. CJM, SJVD, and MEL wrote the paper. ■

### References

- Forster J, Famili I, Fu P, Palsson BO, Nielsen J (2003) Genome-scale reconstruction of the *Saccharomyces cerevisiae* metabolic network. *Genome Res* 13: 244–253.
- Van Dien SJ, Lidstrom ME (2002) Stoichiometric model for evaluating the metabolic capabilities of the facultative methylotroph *Methylobacterium extorquens* AM1, with application to reconstruction of C(3) and C(4) metabolism. *Biotechnol Bioeng* 78: 296–312.
- Reed JL, Vo TD, Schilling CH, Palsson BO (2003) An expanded genome-scale model of *Escherichia coli* K-12 (iJR904 GSM/GPR). *Genome Biol* 4: R54.
- Hartwell LH, Hopfield JJ, Leibler S, Murray AW (1999) From molecular to modular cell biology. *Nature* 402: C47–C52.
- Wolf DM, Arkin AP (2003) Motifs, modules and games in bacteria. *Curr Opin Microbiol* 6: 125–134.
- Aslund F, Beckwith J (1999) The thioredoxin superfamily: Redundancy, specificity, and gray-area genomics. *J Bacteriol* 181: 1375–1379.
- Chistoserdova L, Chen SW, Lapidus A, Lidstrom ME (2003) Methylotrophy in *Methylobacterium extorquens* AM1 from a genomic point of view. *J Bacteriol* 185: 2980–2987.
- Chistoserdova L, Vorholt JA, Thauer RK, Lidstrom ME (1998) C1 transfer enzymes and coenzymes linking methylotrophic bacteria and methanogenic Archaea. *Science* 281: 99–102.
- Vorholt JA, Marx CJ, Lidstrom ME, Thauer RK (2000) Novel formaldehyde-activating enzyme in *Methylobacterium extorquens* AM1 required for growth on methanol. *J Bacteriol* 182: 6645–6650.
- Hagemeyer CH, Chistoserdova L, Lidstrom ME, Thauer RK, Vorholt JA (2000) Characterization of a second methylene tetrahydromethanopterin dehydrogenase from *Methylobacterium extorquens* AM1. *Eur J Biochem* 267: 3762–3769.
- Marx CJ, Laukel M, Vorholt JA, Lidstrom ME (2003) Purification of the formate-tetrahydrofolate ligase from *Methylobacterium extorquens* AM1 and demonstration of its requirement for methylotrophic growth. *J Bacteriol* 185: 7169–7175.
- Marx CJ, Chistoserdova L, Lidstrom ME (2003) Formaldehyde-detoxifying role of the tetrahydromethanopterin-linked pathway in *Methylobacterium extorquens* AM1. *J Bacteriol* 185: 7160–7168.
- Marx CJ, Lidstrom ME (2004) Development of an insertional expression vector system for *Methylobacterium extorquens* AM1 and generation of null mutants lacking *mtaA* and/or *fch*. *Microbiology* 150: 9–19.
- Lidstrom ME (2001) Aerobic methylotrophic prokaryotes. In: Dworkin, M., editor, *The prokaryotes*, 3rd edition, release 3.7. New York: Springer-Verlag. Available: <http://141.150.157.117:8080/prokPUB/index.htm>. Accessed 26 November 2004.
- Kallen RG, Jencks WP (1966) The mechanism of the condensation of formaldehyde with tetrahydrofolic acid. *J Biol Chem* 241: 5851–5863.
- Vorholt JA (2002) Cofactor-dependent pathways of formaldehyde oxidation in methylotrophic bacteria. *Arch Microbiol* 178: 239–249.
- Pomper BK, Saurel O, Milon A, Vorholt JA (2002) Generation of formate by the formyltransferase/hydrolase complex (Fhc) from *Methylobacterium extorquens* AM1. *FEBS Lett* 523: 133–137.
- Chistoserdova L, Laukel M, Portais JC, Vorholt JA, Lidstrom ME (2004) Multiple formate dehydrogenase enzymes in the facultative methylotroph *Methylobacterium extorquens* AM1 are dispensable for growth on methanol. *J Bacteriol* 186: 22–28.
- Chistoserdova LV, Lidstrom ME (1994) Genetics of the serine cycle in *Methylobacterium extorquens* AM1: Identification of *sgaA* and *mtaA* and sequences of *sgaA*, *hprA*, and *mtaA*. *J Bacteriol* 176: 1957–1968.
- Pomper BK, Vorholt JA, Chistoserdova L, Lidstrom ME, Thauer RK (1999) A methenyl tetrahydromethanopterin cyclohydrolase and a methenyl tetrahydrofolate cyclohydrolase in *Methylobacterium extorquens* AM1. *Eur J Biochem* 261: 475–480.
- Attwood MM, Quayle JR (1984) Formaldehyde as a central intermediary metabolite of methylotrophic metabolism. In: Crawford RL, Hanson RS, editors. *Microbial growth on C1 compounds*. Washington, DC: American Society for Microbiology. pp. 315–323.
- Husek P (1991) Amino acid derivatization and analysis in five minutes. *FEBS Lett* 280: 354–356.
- Christensen B, Nielsen J (1999) Isotopomer analysis using GC-MS. *Metab Eng* 1: 282–290.
- Marx CJ, O'Brien BN, Breezee J, Lidstrom ME (2003) Novel methylotrophy genes of *Methylobacterium extorquens* AM1 identified by using transposon mutagenesis including a putative dihydromethanopterin reductase. *J Bacteriol* 185: 669–673.
- Caccamo MA, Malone CS, Rasche ME (2004) Biochemical characterization of a dihydromethanopterin reductase involved in tetrahydromethanopterin biosynthesis in *Methylobacterium extorquens* AM1. *J Bacteriol* 186: 2068–2073.
- Rasche ME, Havemann SA, Rosenzweig M (2004) Characterization of two methanopterin biosynthesis mutants of *Methylobacterium extorquens* AM1 by use of a tetrahydromethanopterin bioassay. *J Bacteriol* 186: 1565–1570.
- Van Dien SJ, Strovas T, Lidstrom ME (2003) Quantification of central metabolic fluxes in the facultative methylotroph *Methylobacterium extorquens* AM1 using <sup>13</sup>C-label tracing and mass spectrometry. *Biotechnol Bioeng* 84: 45–55.
- Roof DM, Roth JR (1988) Ethanolamine utilization in *Salmonella typhimurium*. *J Bacteriol* 170: 3855–3863.
- Reid MF, Fewson CA (1994) Molecular characterization of microbial alcohol dehydrogenases. *Crit Rev Microbiol* 20: 13–56.
- Prosser JJ (1989) Autotrophic nitrification in bacteria. *Adv Microb Physiol* 30: 125–181.
- Ensign SA (2001) Microbial metabolism of aliphatic alkenes. *Biochemistry* 40: 5845–5853.
- Barceloux DG, Bond GR, Krenzelok EP, Cooper H, Vale JA, et al. (2002) American Academy of Clinical Toxicology practice guidelines on the treatment of methanol poisoning. *J Toxicol Clin Toxicol* 40: 415–446.
- Kalyuzhnaya MG, Lidstrom ME (2003) QscR, a LysR-type transcriptional regulator and CbbR homolog, is involved in regulation of the serine cycle genes in *Methylobacterium extorquens* AM1. *J Bacteriol* 185: 1229–1235.
- Anthony C (1990) The oxidation of methanol in gram-negative bacteria. *FEMS Microbiol Rev* 7: 209–214.
- Peel D, Quayle JR (1961) Microbial growth on C<sub>1</sub> compounds: 1. Isolation and characterization of *Pseudomonas* AM1. *Biochem J* 81: 465–469.
- Attwood MM, Harder W (1972) A rapid and specific enrichment procedure for *Hyphomicrobium* spp. *Antonie Van Leeuwenhoek* 38: 369–377.
- Marx CJ, Lidstrom ME (2002) Broad-host-range *cre-lox* system for antibiotic marker recycling in gram-negative bacteria. *Biotechniques* 33: 1062–1067.
- Vorholt JA, Chistoserdova L, Lidstrom ME, Thauer RK (1998) The NADP-dependent methylene tetrahydromethanopterin dehydrogenase in *Methylobacterium extorquens* AM1. *J Bacteriol* 180: 5351–5356.
- Neidhardt FC, Ingraham JL, Schaechter M (1990) *Physiology of the bacterial cell*. Sunderland (Massachusetts): Sinauer. 506 p.